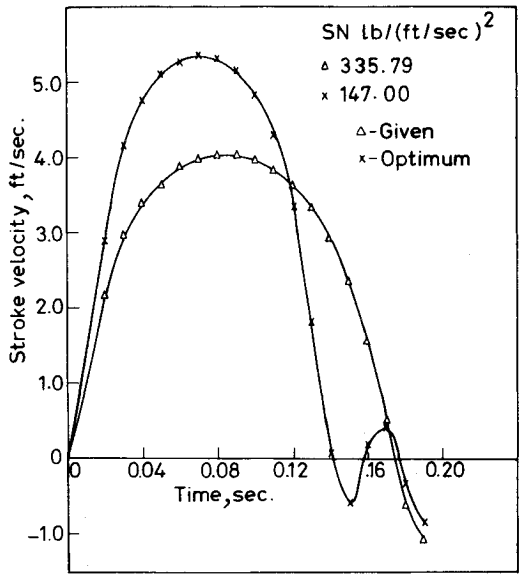

Fig. 3 Stroke velocity vs time. For symbols, see Fig. 1.

the stroke velocity that the velocity increases to a maximum in a small interval of time, drops down to zero, and then changes its sign. Until the stroke velocity reaches its maximum, both the airspring and damping forces increase. Beyond this maximum velocity, airspring force increases at a slower rate, but the damping force decreases. Hence the load keeps on increasing until the stroke velocity reaches its maximum, and then the load decreases. The time of occurrence of peak load depends on the relative magnitudes of the two forces.

At the end of the stroke, when the stroke velocity is zero, the damping force is also zero. Now, only the airspring force is in action trying to extend the shock absorber. Therefore, the load decreases after that instant. The valley in between the two peaks is determined by the magnitudes of the airspring force that is increasing and the damping force that is decreasing.

Conclusion

In the transient of the ground load of an aircraft, there are two peaks, the relative magnitudes of which depend on the damping constant of the shock absorber. In the optimum damping case, the magnitudes of the peaks are almost the same.

Hence, by looking at the transient response of the ground load of an aircraft while landing, we can judge whether the damping constant of the shock absorber is optimal. If the first peak value is greater than the second peak value, decrease the damping constant (by increasing the area of the orifice) to reach the optimum; if the second peak value is greater, increase the damping constant (by decreasing the area of the orifice) to obtain the optimum. The extent of the required change in the orifice area depends on the relative magnitudes of the two peaks. In the opinion of the author, the above result could be used as a rule of thumb for the optimum design of an aircraft undercarriage.

Acknowledgment

The author wishes to thank A. K. Rao and R. Krishnan of the Indian Institute of Science, Bangalore, and R. Sankaranarayanan and V. T. Nagaraj of Hindustan Aeronautics Limited, Bangalore, for their guidance and support in carrying out this work.

References

[1] Yff, J., "Analysis of Dynamic Aircraft Landing Loads and a Proposal for Rational Design Landing Load Requirements," Ph.D. Dissertation, June 27, 1972, Technische Hogeschool, Delft, Netherlands.

[2] Himmelblau, D. M., *Applied Nonlinear Programming*, McGraw-Hill, New York, 1972.

[3] Milwitzky, B. and Cook, F. C., "Analysis of Landing Gear Behavior," NACA Report 1154, 1953.

[4] Venkatesan, C., "Optimum Design of an Aircraft Undercarriage System," report submitted to Hindustan Aeronautics Ltd., Bangalore, India, Nov. 1976.

[5] McGhee, J. R., and Carden, H. D., "A Mathematical Model of an Active Control Landing Gear for Load Control during Impact and Roll-Out," NASA TND 8080, Feb. 1976.

Evaluation of Flight Spoilers for Vortex Alleviation

Delwin R. Croom*
NASA Langley Research Center, Hampton, Va.

Nomenclature

$C_{L,\text{trim}}$ = trimmed lift coefficient of generating model
$C_{l,TW}$ = trailing wing rolling-moment coefficient

$$\frac{\text{trailing wing rolling moment}}{qS_{TW}b_{TW}}$$

q = dynamic pressure at trailing wing location
S_{TW} = area of trailing wing
b_{TW} = span of trailing wing

Introduction

THE strong vortex wakes generated by large transport aircraft are a potential hazard to smaller aircraft, and so NASA is involved in a program of model tests, flight tests, and theoretical studies to determine the feasibility of reducing this hazard by aerodynamic means.

The magnitude of the vortex-wake hazard is influenced greatly by the direction of the flight of the aircraft which is penetrating the trailed vortices. A cross-track penetration at right angles to the trailing vortices tends to cause pitching and vertical motion and to produce vertical loads on the penetrating airplane in a manner similar to that of a gust encounter. Also, an along-track penetration, parallel to and between the wingtip vortices, can occur in both the takeoff climbout and the landing approach. This type of penetration may cause settling or, at least, may reduce the rate of climb of the penetrating aircraft. However, an along-track penertration through the vortex center is considered to be the most hazardous encounter since such penetration induces a rolling motion to the penetrating aircraft that could result in an upset.

The approach being used by NASA to evaluate the effectiveness of vortex-alleviation devices in ground-based facilities is to simulate an airplane flying in the trailing vortex of another larger airplane and to make direct measurements of rolling moments induced on the trailing model by the vortex generated by the forward model. From flight tests, the pilot's qualitative separation requirement is determined from the separation distance where the vortex-induced upset would cause a missed approach during an IFR landing.

This Note briefly summarizes the results obtained to date from wind-tunnel and full-scale flight investigations of the flight spoilers that exist on the wide-bodied transport jet aircraft when used as trailing vortex hazard alleviation devices. All of the data presented herein were obtained with

Received Jan. 14, 1977; revision received Feb. 24, 1977.
Index categories: Aerodynamics; Flight Operations; Jets, Wakes, and Viscid-Inviscid Flow Interactions.
*Senior Aeronautical Engineer.

the vortex generating models at a trimmed lift coefficient of 1.2.

Models and Apparatus

Transport aircraft models used in these investigations in the NASA Langley V/STOL tunnel were a 0.03-scale B-747 model, a 0.047-scale DC-10-30 model, and a 0.05-scale L-1011 model. The B-747 model and the L-1011 model were sting-mounted; the DC-10-30 model was strut-mounted. A six-component internal strain-gage balance was used to measure forces and moments. The trailing wing models used in these investigations were unswept and had a span and aspect ratio typical of a small-size transport aircraft (Learjet). The trailing wing models were mounted on a single-component, strain-gage roll balance which was attached to a traverse mechanism capable of moving the model both laterally and vertically. This entire traverse mechanism could be mounted to the tunnel floor at various tunnel longitudinal positions downstream of the transport aircraft models. A more complete description of the transport aircraft models and trailing wing models is given in Refs. 1-3.

The Langley V/STOL tunnel has a test section height of 4.42 m, a width of 6.63 m, and a length of 15.24 m. All tests were run at a freestream dynamic pressure in the tunnel test section of 430.9 Pa, which corresponds to a velocity of 27.4 m/sec.

Discussion

Figure 1 is a sketch of the flight spoilers on the B-747 aircraft. These spoilers normally are operated symmetrically for air and ground speed brakes and unsymmetrically for lateral control. For this investigation, various combinations of the segments of these spoilers were deflected symmetrically. Combinations of spoiler segments investigated were 1) segments 1 and 2, 2) segments 2 and 3, 3) segments 3 and 4, and 4) segments 1 and 4.

The induced rolling-moment coefficient on the trailing wing model measured at several downstream distances behind the B-747 airplane model, with various segments of flight spoilers deflected to 45°, are shown in Fig. 2. It can be seen in Fig. 2 that all combinations of flight spoilers investigated on the B-747 airplane model were effective in reducing the induced rolling moment on the trailing wing model by as much as 40 to 50% at all downstream distances investigated. Of particular interest is the ability of these devices to effect a large reduction in maximum trailing wing rolling-moment coefficient $(C_{l,TW})_{max}$ (50 to 70%) in the relative near distances (about seven B-747 wingspans) downstream of the B-747 aircraft model. Complete results of this investigation are given in Ref. 1.

As a result of the findings in the ground-based facilities, a flight program was conducted at the Hugh L. Dryden Flight Research Center which used the existing flight spoilers on a NASA-owned B-747 airplane as the vortex attenuating device.[4] A T-37 airplane was used to penetrate the trailing vortex. The trailing vortex wake was made visible by smoke. Penetrations behind the B-747 aircraft in its landing configuration on a 3° flight path were limited to about 7 miles. (Pilots qualitative separation requirement was 9 miles.) With

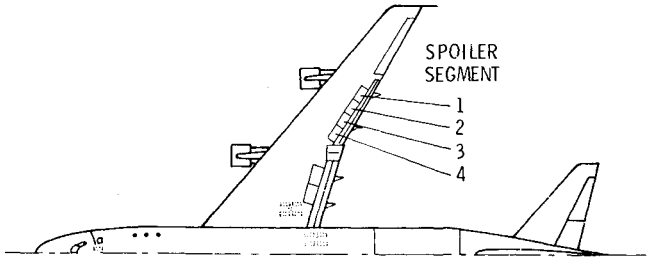

Fig. 1 Sketch of flight spoilers on the B-747 airplane.

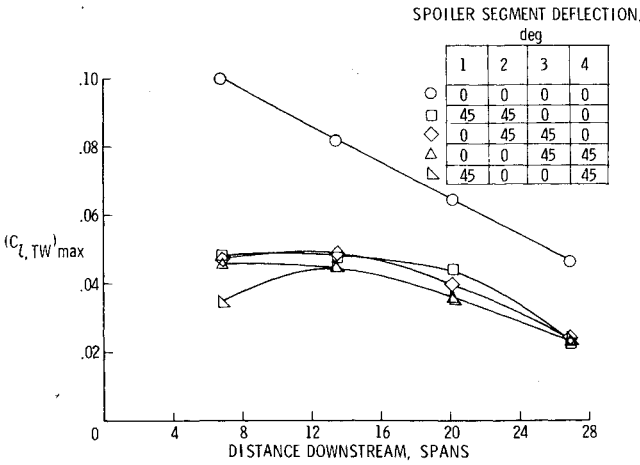

Fig. 2 Variation of trailing wing rolling-moment coefficient with downstream distance behind the B-747 airplane model with various segments of the flight spoilers deflected 45°. Landing flap configuration, $C_{L,trim} = 1.2$.

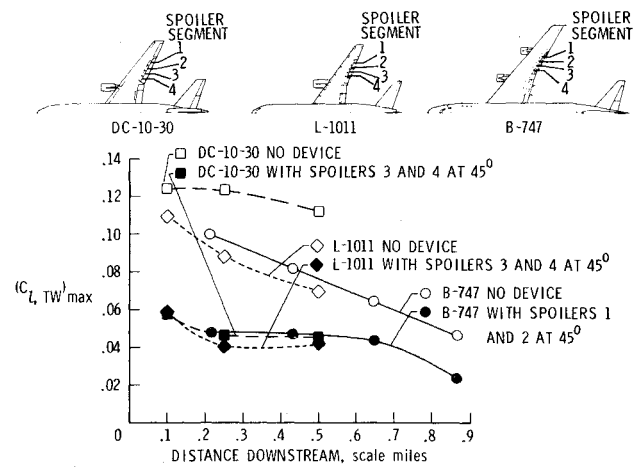

Fig. 3 Variation of trailing wing rolling-moment coefficient with downstream distance behind the B-747, DC-10-30, and L-1011 airplane models with and without spoiler trailing vortex alleviators. Landing flap configuraiton, $C_{L,trim} = 1.2$.

appropriate deflection of the B-747 flight spoilers, penetration as close as about 1.5 miles were made. (Pilots qualitative separation requirement was about 3 miles.) These flight results have verified the trends obtained in the ground-based facilities.

The other two American wide-bodied jet transport airplanes (DC-10 and L-1011) have flight spoilers that are located forward of the outboard flaps similar to those on the B-747 airplane. Models of both of these airplanes were made available to NASA by the respective aircraft companies at no cost to the Government for tests in the Langley V/STOL tunnel. Spoiler segment combinations 1 and 2, 2 and 3, 3 and 4, and 1 and 4 were investigated on both the DC-10-30 and L-1011 airplane models. Results of the DC-10-30 model tests are presented in Ref. 2. Results of the L-1011 model tests are presented in Ref. 3.

A comparison of the effectiveness of the flight spoilers on all of the wide-bodied transport configurations investigated in reducing the induced rolling moment on the trailing wing model is shown in Fig. 3. The attenuated $(C_{l,TW})_{max}$ values obtained with flight spoiler segments 3 and 4 on both the DC-10-30 and L-1011 airplane models in the landing flap configuration are comparable with the attenuated values of $(C_{l,TW})_{max}$ obtained in wind-tunnel test of the B-747 airplane model in its landing flap configuration. Since flight spoilers were shown to be effective in attenuating the trailing vortex in

full-scale flight tests of the B-747 airplane, it is expected that the use of flight spoilers on both the DC-10-30 and L-1011 airplanes also would be effective in attenuating the trailing vortex behind both of these airplanes.

Concluding Remarks

Based on the results obtained in these investigations, it was found by ground-based tests and verified by full-scale flight tests that the existing flight spoilers on the B-747 airplane are effective as trailing vortex attenuators. Based on the results of wind-tunnel investigations of the DC-10-30 and L-1011 airplane models, the existing flight spoilers on both the DC-10-30 and L-1011 airplanes are also expected to be effective trailing vortex attenuators.

References

[1] Croom, D. R., "Low-Speed Wind-Tunnel Investigation of Various Segments of Flight Spoilers as Trailing-Vortex-Alleviation Devices on a Transport Aircraft Model," NASA TN D-8162, 1976.

[2] Croom, D. R., Vogler, R. D., and Thelander, J. A., "Low-Speed Wing-Tunnel Investigation of Flight Spoilers as Trailing-Vortex-Alleviation Devices on an Extended Range Wide-Body Tri-Jet Airplane Model," NASA TN D-8373, 1976.

[3] Croom, D. R., Vogler, R. D., and Williams, G. M., "Low-Speed Wind-Tunnel Investigation of Flight Spoilers as Trailing-Vortex-Alleviation Devices on a Medium-Range Wide-Body Tri-Jet Airplane Model," NASA TN D-8360, 1976.

[4] Barber, M. R., Hastings, E. C. Jr., Champine, R. A. and Tymczyszyn, J. J., "Vortex Attenuation Flight Experiment," NASA SP-409, Wake Vortex Minimization, 1976.

Consideration of Clogging in Boundary-Layer Control System Design

Peter Crimi*
Avco Systems Division, Wilmington, Mass.

Introduction

BOUNDARY-LAYER control systems that employ suction through perforated or porous surfaces are subject to clogging by airborne sand and dust particles. Critics of boundary-layer control have often cited this problem as a serious limitation to practical application of boundary-layer control.[1] An analysis was undertaken to define the principal parameters affecting the clogging problem and to determine whether clogging could be alleviated or eliminated through proper design. A model for the clogging mechanism has been developed, the primary parameters of which are perforation size, particle size, boundary-layer thickness and velocity profile, external flow static and dynamic pressures, and suction pressure. Two different applications of boundary-layer control were analyzed, and design limitations to avoid clogging of systems used to prevent leading-edge stall have been delineated. Consideration has been directed specifically to systems employing perforations. The results obtained should also be applicable, however, at least qualitatively, to systems using porous surfaces made, for example, from sintered metals.

Received Feb. 23, 1977; revision received April 20, 1977.

Index categories: Subsystem Design; Boundary Layers and Convective Heat Transfer – Laminar; Boundary Layers and Convective Heat Transfer – Turbulent.

*Senior Consulting Scientist.

Model for Clogging

Consider, as an analogue of the physical problem, a spherical particle of diameter D_p lodged in a circular hole of diameter D_h, as sketched in Fig. 1. The particle is subjected to a shear flow, either laminar or turbulent, in which the magnitude of the fluid velocity is denoted $U(y)$. The portion of the sphere inside the hole is subjected to suction pressure p_s, which is necessarily less than the pressure p_e of the external flow.

The lift on the particle is assumed to be negligible in comparison to the force due to suction pressure. To evaluate the drag on the particle, it is first assumed that the drag coefficient C_D of the exposed portion, for a uniform freestream, is the same as that of a complete sphere. This is a reasonable assumption, since a hemisphere and a sphere have very nearly the same drag coefficient, provided projected area normal to the flow is used as reference area. It is further assumed that the drag per unit height on a horizontal section of the particle, denoted $d(y)$, is a weighted fraction of the total drag, using the product of U^2 and local width $b(y)$ as weighting function. Thus

$$d(y) = C_D \frac{\rho}{2} U^2(y) b(y) \tag{1}$$

This strip, or slab, formulation is similar to the method used to evaluate drag on buildings subjected to wind shear, whereby the mean value, over the height of the building, of the dynamic pressure is substituted in the expression for the drag.[2]

The limiting condition for no clogging of an individual particle is achieved when the moment due to drag about the furthest downstream contact point is just sufficient to overcome the moment due to the suction on the portion of the particle in the hole. This condition is expressed analytically by

$$\frac{(p_e - p_s)_{\max}}{q_e} = \frac{16 C_D}{\pi D_h^3} \int_0^h y b(y) \left(\frac{U}{U_e}\right)^2 dy \tag{2}$$

where U_e and p_e are the velocity and pressure in the external flow, respectively, and

$$q_e = \tfrac{1}{2}\rho U_e^2$$

$$h = \tfrac{1}{2}\left[D_p + \sqrt{D_p^2 - D_h^2}\right]$$

$$b = 2\sqrt{\left(\frac{D_p}{2}\right)^2 - \left(y - h + \frac{D_p}{2}\right)^2}$$

and ρ is the air density. Actual boundary-layer velocity profiles, either measured or calculated, could presumably be used in Eq. (2) to obtain the limiting condition. For present purposes, though, it was felt that the following approximations, taken from Ref. 3, would suffice:

Laminar	Turbulent
$\frac{U}{U_e} = \frac{2y}{\delta} - 2\left(\frac{y}{\delta}\right)^3 + \left(\frac{y}{\delta}\right)^4$	$\frac{U}{U_e} = \left(\frac{y}{\delta}\right)^{1/7}$ $y < \delta$
$\frac{U}{U_e} = 1$	$\frac{U}{U_e} = 1$ $y \geq \delta$
$\delta^*/\delta = 0.3$	$\delta^*/\delta = 0.125$

where δ^* is displacement thickness. A value of 0.4 was assigned to C_D for all calculations.

Applications to Specific Systems

Suction Limit for No Clogging

Two parameters define the limiting suction value prescribed by Eq. (2), namely, D_p/D_h and D_h/δ^*. For a given value of